JTE HCMUTE
ISSN: 2615-9740

JOURNAL OF TECHNICAL EDUCATION SCIENCE
Ho Chi Minh City University of Technology and Education
Website: https://jte.edu.vn/
Email: jte@hcmute.edu.vn

Investigating the Antibacterial Activities of Graphene Oxide Loaded Spiky Gold Nanocomposites via Chitosan linker

Tam Minh Le, Nhung Thi Tran*
Ho Chi Minh City University of Technology and Education, Vietnam

*Corresponding author. *Email: nhungtt@hcmute.edu.vn*

ARTICLE INFO

Received:	18/10/2023
Revised:	14/11/2023
Accepted:	15/11/2023
Published:	28/12/2023

KEYWORDS

Spiky Gold nanoparticles;
Graphene oxide;
Nanocomposites;
Antibacterial;
Plasmon-induced thermal.

ABSTRACT

The graphene oxide (GO) loaded spiky gold (AuNS) nanocomposites were prepared by electrostatic interaction between negatively-charged GO nanosheets and positively-charged AuNS by the assistance of chitosan as linker molecules. The AuNS/GO nanocomposites exhibit a red-shift in the extinction spectra and a reduction in the zeta potential compared to those of the pristine AuNS due to the presence of oxygen-containing functional groups in GO. The bactericidal analysis demonstrates that the incorporation of GO greatly enhances the intrinsic antibacterial activities of AuNS. Besides, the AuNS with smaller size exhibit better bactericidal efficiency compared to that of AuNS with bigger size. Upon light irradiation, the AuNS/GO with the absorption peak close to the wavelength of excitation light (900 vs. 904 nm) demonstrates a noticeable improvement in the bactericidal efficiency which is attributed to the plasmon-induced photothermal effect. All these results suggest that the AuNS/GO nanocomposites can work as a promising functional material for both intrinsic and plasmon-induced antibacterial materials.

Doi: https://doi.org/10.54644/jte.80.2023.1484

1. Introduction

Metal and metal oxide nanoparticles are well-known for their intrinsic antibacterial properties which are attributed to their ability to: (1) release metal ions to poison the cell metabolism mechanism, (2) adhere and disrupt the cell membrane through physical interaction, (3) generate reactive oxygen species [1], [2]. The antibacterial activities of metallic nanoparticles are determined by their size, shape, composition, and crystallography. Within different morphology-engineered nanoparticles, spiky gold nanoparticles (AuNS) with multiple sharp tips have received great consideration. These sharp tips can readily anchor to cell membrane and thus killing the bacterial more efficiently. The spiky gold nanoparticles with multiple sharp tips have been demonstrated to exhibit an improved bactericidal efficacy compared to that of other morphology-engineered nanoparticles [3], [4].

In addition, graphene oxide, a derivative of graphene with C sp^2 honeycomb structure enriched with oxygen-containing functional groups was widely used as templates in the aqueous synthesis of metallic nanocomposites [5]. The large surface area combined with sharp edges/ corners endows GO antibacterial activities toward various types of bacteria. The nanocomposites of GO and other metal and metal oxide nanoparticles including Ag, Au, ZnO, TiO_2… have been prepared and demonstrated improved antibacterial properties compared to pristine materials [6]-[8]. Normally, metallic nanoparticles are anchored onto GO nanosheets by the in-situ synthesis or via linker molecules. Compared to the in-situ synthesis, the later method enables the well control over the size, shape, and optical properties of the attached nanoparticles. Herein, we used chitosan, a product of the de-acetylation of chitin as linker molecules. In addition, chitosan also works as capping agent to stabilize the spiky gold nanoparticles in the synthesis protocol. Despite its dual functions, chitosan was also reported to possess antibacterial properties due the presence of amine groups; thereby, the antibacterial activities of AuNS/GO nanocomposites was further enhanced [9].

Furthermore, the plasmon-induced themal effect of plasmonic nanoparticles have been reported to improve the bacterial killing and cancer treatment performance [10]. The effect of radiation on the bacterial killing efficiency of the AuNS/GO nanocomposites was also investigated, in which two types of spiky AuNS nanoparticles with the absorbance peaks close and far from the wavelength of the excitation light were selected. The AuNS/GO nanocomposites with the absorbance wavelength close to the excitation wavelength demonstrate better antibacterial activities, suggesting the intrinsic and plasmon-induced antibacterial properties of the AuNS/GO nanocomposites via chitosan as linker molecules.

2. Materials and Methods

2.1. Materials

Gold (III) chloride hydrate $HAuCl_4.x\ H_2O$ (~ 52 % basis), Silver nitrate $AgNO_3$ (99 %), Ascorbic acid (99%) were purchased from Sigma Aldrich. Chitosan with the deacetylation ≥ 75% was purchased from Himedia, India. Other chemicals were purchased from local brands. All chemicals were used as reagent grade without purification.

2.2. Methods

All glassware was washed intensively with aqua regia solution (HCl: HNO_3 = 3: 1 v/v) and double distilled water before using.

Synthesis of spherical gold nanoparticles (AuNPs): The AuNPs were synthesized based on our previous protocol. In details, 1.525 mL $HAuCl_4$ (10 mM) was added into an Erlen containing 55.475 mL double-distilled water under magnetic stirring. The solution was heated to boiling. Subsequently, 3 mL trisodium citrate (10 mg/mL) was quickly added. The color of the above solution gradually changed from colorless to light pink and wine red within 25 minutes of vigorous stirring. Afterwards, the heater was removed and the as-prepared AuNPs dispersion was gently stirred under ambient condition until it cooled to room temperature. Finally, double distilled water was added to adjust the concentration of gold nanoparticles at 0.5 mM (correlated to the Au^{3+} content). The spherical AuNPs dispersion was kept in refrigerator at 4 °C.

Synthesis of spiky gold nanoparticles (AuNS): the spiky gold nanoparticles was prepared based on seed-mediated growth approach which was previously reported with modification [11], [12]. In a typical protocol, an aliquot amount of AuNPs seeds were added into a vial containing 270 µL $HAuCl_4$ (10 mM), 75 µL $AgNO_3$ (10 mM), 45 µL HCl 1M under magnetic stirring. Afterward, 225 µL ascorbic acid (10 mg/mL) was quickly added to trigger the formation of spiky AuNS. The color of the suspension was rapid changed to blue. After 2 min of vigorous stirring, 1.315 mL chitosan 10 mg/mL was slowly added. The resultant dispersion was kept stirring for further 30 minutes. Finally, the AuNS dispersion was rinsed thoroughly by centrifuging at 8000 rpm in 20 minutes and discarding with double distilled water. This steps were repeated for two times.

Synthesis of spiky gold nanoparticles loaded on GO nanosheets to form AuNS/GO nanocomposites: the electrostatic force between amino groups on the surface of AuNS and oxygen-containing functional groups on GO was exploited to anchor AuNS onto GO nanotemplates. Typically, 1 mL of AuNS dispersion was added into a centrifugation tube containing 3 mL double distilled water. Afterward, 0.95 mL GO (1 mg/mL) was rapidly added. The suspension was sonicated in a sonication bath for 5 minutes and kept undisturbed overnight to achieve the equilibrium state.

Antibacterial activity analysis: The *Escherichia coli* (VTCC-B-482) was provided by the Institute of Microbiology and Biotechnology, Hanoi National University. The cfu counting technique were chosen to estimate the number of viable bacteria after incubation with various amounts of AuNS and AuNS/GO samples. In a typical protocol, the bacterial suspension (10^3 Cfu/ mL) was incubated in the presence of various concentrations of as-prepared AuNS and AuNS/GO nanocomposites (2, 5, 10 µg/ mL) for 10 minutes. After that, 100 µL of the bacterial suspension of each investigated sample was spread onto an agar plates. The agar plates were then cultured at 37 °C for 24 hours to analyze the number of viable bacteria. To investigate the effect of light, the 904 nm light was irradiated to the bacterial suspension during the incubation process prior to spreading on agar plates. All the control samples were conducted in the same manner for comparison. Noted that, all tools, equipment, and chemicals for the antibacterial activity examination were sterilized for 40 minutes at 121°C and 0.26 MPa in a high-pressure steam sterilization pot (Yamato, SQ510, Japan). All experiments were repeated three times. The percentage of killed bacteria H (%) was calculated by:

$$H(\%) = 100 - \frac{number\ of\ viable\ bacteria\ in\ each\ investigated\ sample}{number\ of\ viable\ bacteria\ in\ the\ control\ sample} \times 100$$

2.3. Characterization

The morphology of the as-synthesized nanoparticles was characterized by transmission microscopy spectrometer (JEM-1010) operated at 120 kV accelerating voltage, the optical properties were analyzed by UV-Vis spectrometer (UH5300, Hitachi), the Zeta potentials were recorded by Zetasizer (Malvern).

3. Results and Discussion

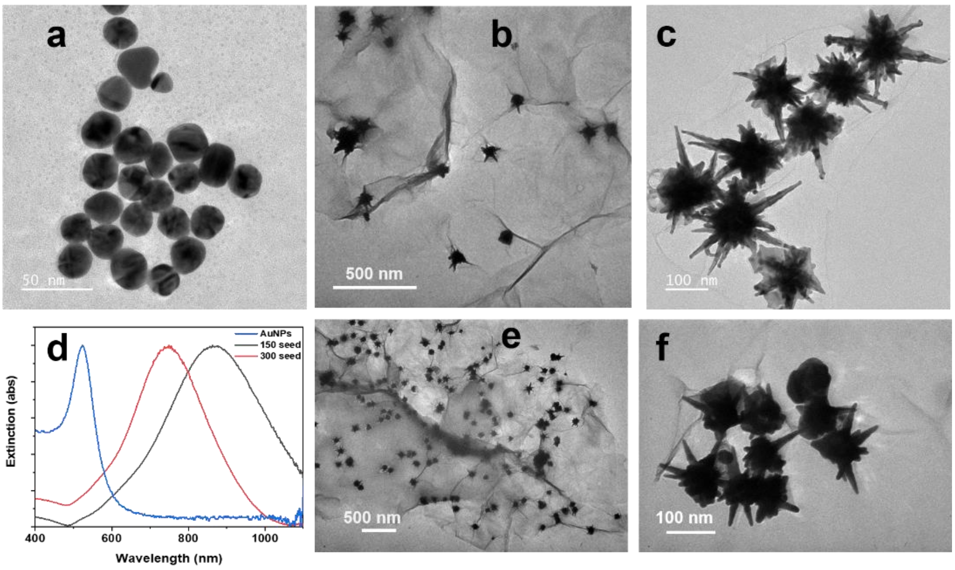

Figure 1. *(a) TEM images of spherical AuNPs, (b, c) TEM image of AuNS/GO-150 nanocomposites, (d) UV-Vis spectra of AuNPs and spiky AuNS-150, AuNS-300 nanoparticles, (e, f) TEM images of AuNS/GO-300 nanocomposites.*

The spherical gold nanoparticles (AuNPs) exhibit a uniform size distribution of 20 ~ 30 nm in diameter, Figure 1a. A sharp extinction peak was observed at abt. 520 nm which is a typical plasmon peak of Au nanospheres, Figure 1d. The spherical AuNPs were used as seed particles to facilitate the formation spiky gold nanoparticles (AuNS) with a few sharp tips extruding from central cores via a seed-mediated growth approach, Figure 1c-f. The optical responses of the as-synthesized AuNS was facilely controlled by tailoring the amount of added AuNPs seeds, Figure 1d. A blue-shift in the extinction peak position from 890 to 750 nm was observed upon increasing the doses of AuNPs seeds from 150 to 300 µL, so-called AuNS-150 and AuNS-300 nanoparticles, respectively. According to literature, the optical properties of branched Au nanostructures is governed by their particle size, their composition, the number of tips and the tip length. Therefore, a lower amount of seeds adding generated AuNS with bigger size and longer tips, Figure 1c-f. As a result, their spectral peak position shifted to shorter wavelength, Figure 1d. To prepare the AuNS/GO nanocomposites, herein, chitosan a polysaccharide obtained from the de-acetylation of chitin was used as both capping and linker agents. At first, the freshly-prepared AuNS were stabilized by encapsulating with chitosan. The presence of abundant amino groups on the structure of chitosan endows the surface of AuNS with positive charge. Afterward, the chitosan-modified AuNS was loaded on the surface of GO sheets via electrostatic interaction between positively-charged amino groups on chitosan and negatively-charged functional groups on GO. Graphene oxide, a derivatives of graphene, with numerous oxygen-containing functional groups on the structure was widely exploited as templates in the aqueous synthesis of metallic nanocomposites. The TEM images of AuNS-150 and AuNS-300 nanoparticles loaded on GO nanosheets were displayed in Figure 1b-c and 1e-f, respectively. The observed wrinkles in TEM images is attributed to the presence of GO nanosheets. From the TEM analysis, the AuNS was found to evenly distributed onto GO nanosheets.

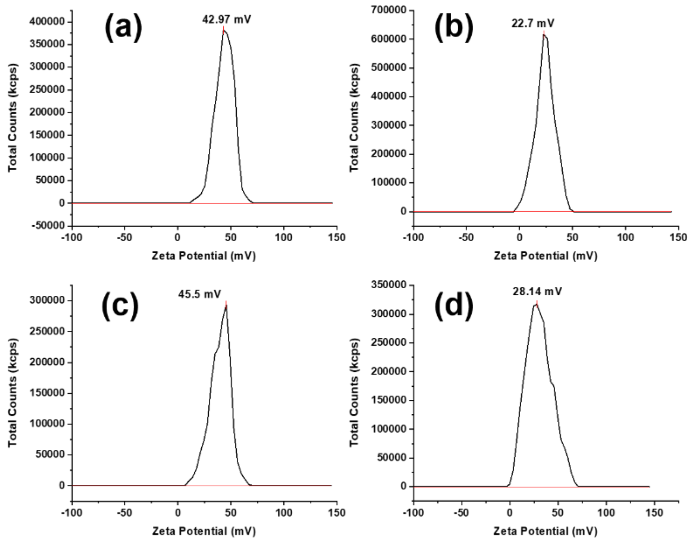

Figure 2. *Zeta potentials of (a, b) AuNS-150 and AuNS/GO-150 nanocomposites, (c, d) AuNS-300 and AuNS/GO-300 nanocomposites.*

To confirm the binding of AuNS onto GO templates, we have recorded the zeta potentials of AuNS before and after incorporation with GO and shown in Figure 2. It is interesting that, without GO, the surface of AuNS exhibit positively-charged zeta potentials of 42.97 and 45.5 mV for AuNS-150 and AuNS-300 nanoparticles, respectively. The positively-charged surface of AuNS is accounted for the presence of numerous amino groups in chitosan. After coating on GO templates, the zeta potentials of the AuNS/GO composites decrease to 22.7 and 28.14 mV for AuNS/GO-150 and AuNS/GO-300, respectively. The reduction in the zeta pontential of the AuNS/GO nanocomposites is definitely due to the neutralization of oxygen-containing functional groups in GO. This finding clearly demonstrates the successful binding of AuNS onto GO nanosheets.

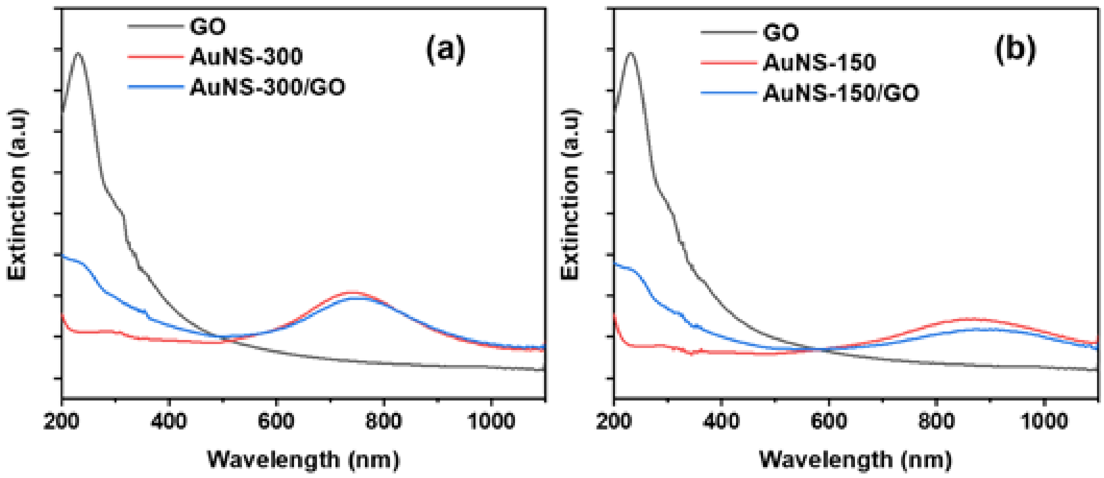

Figure 3. *The UV-Vis spectra of (a) GO, AuNS-300, AuNS/GO-300 nanocomposites and (b) GO, AuNS-150, AuNS/GO-150 nanocomposites.*

The optical response of the AuNS before and after loading onto GO nanosheets was also investigated and shown in Figure 3. It is well-known that the localized surface plasmon resonance (LSPR) response of metallic nanoparticles is determined by their size, shape, topography, composition and the environmental refractive index [13]. The plasmon peak positions of the AuNS shifted to longer wavelengths upon encapsulating with GO nanosheets, (740 to 752 nm for AuNS-300 and AuNS/GO-

300 nanocomposites, and 880 to 900 nm for AuNS-150 and AuNS/GO-150 nanocomposites, respectively). It is attributed to the change in the refractive index after incorporating AuNS onto GO nanosheets. This result again demonstrates the successful loading of AuNS by GO nanosheets.

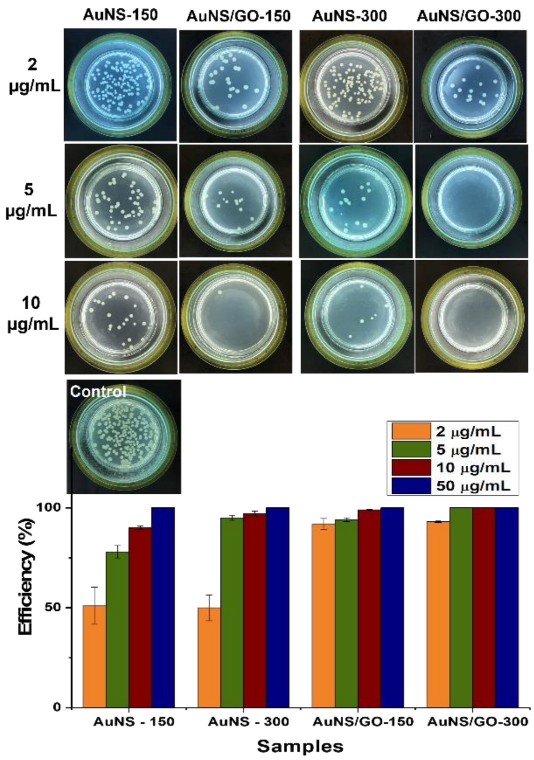

Figure 4. *The photos of incubated disks and the calculated bacterial killing efficiency (%) when E. coli bacteria were in contact with different doses of spiky AuNS and AuNS/GO nanocomposites, respectively.*

The antibacterial properties of the as-prepared AuNS/GO nanocomposites against *E. coli* bacteria were analyzed and shown in Figure 4. All the investigated samples exhibit great bactericidal performances against *E. coli* at low concentrations down to 2 µg/mL. It is reasonable that the killing efficiency increases upon increasing the doses of incubated nanoparticles from 2-10 µg/mL. A better killing yield was observed for the AuNS-300 compared to that of the AuNS-150 nanoparticles which can be accounted for their smaller size. Noteworthy, a great bactericidal improvement was observed for the AuNS/GO nanocomposites at 2 µg/mL incubated dose compared to that of pristine AuNS. The GO with sharp edges can readily adhere to the bacteria cell membrance and thus improve the bacterial killing efficiency. In addition, the synergistic effect generated by the combination of GO and AuNS might be responsible for the better bactericidal activities [6].

The plasmon-induced photothermal effect is induced when the wavelength of radiated light closely matches the surface plasmon resonance peak of plasmonic nanoparticles. To investigate the effect of light irradiation on the bacterial killing efficacy of the AuNS and AuNS/GO nanostructures, the NIR light of 904 nm in wavelength was chosen to ensure the matching with the plasmon peak of the AuNS-150 (abs. 880 nm) and the mis-match with the plasmon peak of the AuNS-300 nanoparticles (abs. 740 nm), respectively, Figure 5. The intensity of the radiated light is adjusted to avoid the heating effect that can kill bacteria. Therefore, there is no change in the number of viable bacteria in the presence/ absence of radiation light for the control sample. It is interesting that all samples exhibit a slight increase in the bactericidal efficiency under light irradiation. However, a notable improvement was observed only for the AuNS/GO-150 nanocomposites. The wavelength matching between the radiated light and AuNS/GO-150 nanoparticles (904 vs. 900 nm) facilitates the plasmon-induced thermal effect. In addition, the oscillating electron pool in GO with C sp^2 honeycomb structure helps improve and dissipate the induced heat throughout AuNS/GO nanocomposites. As a result, the antibacterial efficiency is enhanced.

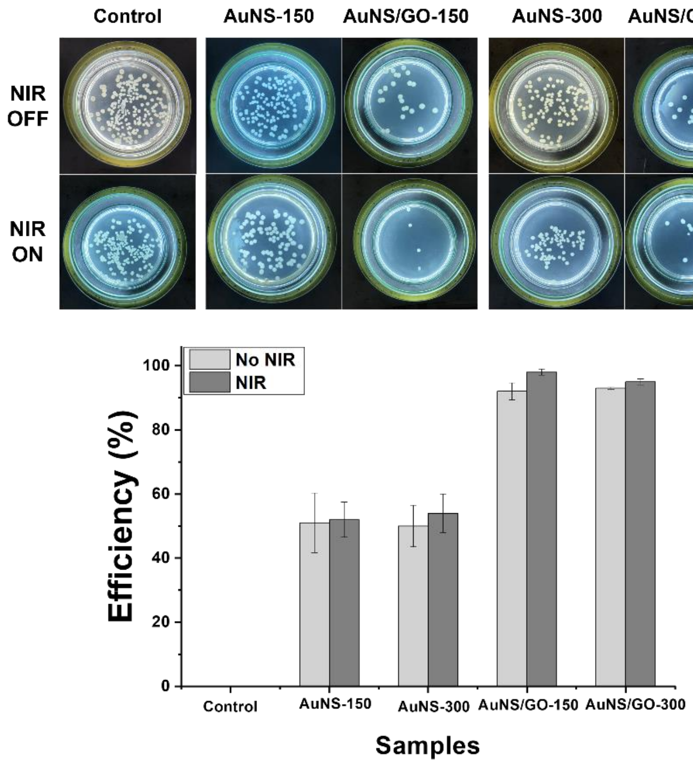

Figure 5. *The photos of incubated disks and calculated bacterial killing efficiency (%) of spiky AuNS and AuNS/GO nanocomposites in the presence/ absence of NIR irradiation.*

4. Conclusions

To summarize, we have successfully prepared AuNS/GO nanocomposites via the chitosan as both stabilizing and linking agents. The zeta potential analysis and the red-shift in their absorbance peak positions suggest the successful binding of AuNS onto GO nanosheets. From our results, we found that the antibacterial activities of the AuNS was greatly improved by the combination with GO nanosheets. Furthermore, the plasmon-induced thermal effect under light radiation with appropriate wavelength also suggests a huge potential to improve the antibacterial activities of metallic nanoparticles. However, the impact of the light intensity and the generated temperature profile on the antibacterial killing efficiency still requires more investigation.

Acknowledgments

The authors would like to thank Ho Chi Minh City University of Technology and Education (HCMUTE) for financial support. The authors also sincerely thank Dr. Thanh-Binh Nguyen, Ms. M. N. T. Nguyen and Ms. Y. L. H. Nguyen for their help.

Conflict of Interest

The authors declare that there is no conflict of interest.

REFERENCES

[1] N. T. Tran *et al.*, "Highly branched and hollow gold nanourchins for bacterial killing and off-resonance SERS sensing," *Chem. Pap.*, vol. 77, pp. 7505-7514, 2023.

[2] X. Gu *et al.*, "Preparation and antibacterial properties of gold nanoparticles: A review," *Environ. Chem. Lett.*, vol. 19, pp. 167-187, 2021.

[3] A. J. Blanch, M. Döblinger, and J. R. Fernández, "Simple and rapid high-yield synthesis and size sorting of multibranched hollow gold nanoparticles with highly tunable NIR plasmon resonances," *Small*, vol. 11, no. 35, pp. 4550-4559, 2015.

[4] P. Ray, T. Lodha, A. Biswas, T. K. Sau, and C. V. Ramana, "Particle-specific physical and chemical effects on antibacterial activities: A comparative study involving gold nanostars, nanorods, and nanospheres," *Colloids and Surfaces A: Physicochemical and Engineering Aspects*, vol. 634, p. 127915, 2022.

[5] N. T. Tran, T. L. Nguyen, H. T. D. Nguyen, T. N. Tu, and V. C. Hoang, "One-pot, green and surfactant-less synthesis of polyhedral PdNPs anchored on GO as a superior catalyst for the reduction of 4-nitrophenol," *Synthetic Metals*, vol. 282, p. 116957, 2021.

[6] Y. Feng *et al.*, "Reduced graphene oxide functionalized with gold nanostar nanocomposites for synergistically killing bacteria through intrinsic antimicrobial activity and photothermal ablation," *ACS Appl. Bio Mater.*, vol. 2, no. 2, pp. 747-756, 2019.
[7] W. Ma *et al.*, "Synthesis and characterization of ZnO-GO composites with their piezoelectric catalytic and antibacterial properties," *Journal of Environmental Chemical Engineering*, vol. 10, no. 3, p. 107840, 2022.
[8] Y. N. Chang *et al.*, "Synthesis of magnetic graphene oxide–TiO2 and their antibacterial properties under solar irradiation," *Applied Surface Science*, vol. 343, pp. 1-10, 2015.
[9] J. Li and S. Zhuang, "Antibacterial activity of chitosan and its derivatives and their interaction mechanism with bacteria: Current state and perspectives," *European Polymer Journal*, vol. 138, p. 109984, 2020.
[10] Y. Liu, B. M. Crawford, and T. V. Dinh, "Gold nanoparticles-mediated photothermal therapy and immunotherapy," *Immunotherapy*, vol. 10, no. 13, pp. 1175-1188, 2018.
[11] J. Ma *et al.*, "Bimetallic core–shell nanostars with tunable surface plasmon resonance for surface-enhanced Raman scattering," *ACS Appl. Nano Mater.*, vol. 3, no. 11, pp. 10885-10894, 2020.
[12] H. Wang, Z. Song, S. Li, Y. Wu, and H. Han, "One stone with two birds: functional gold nanostar for targeted combination therapy of drug-resistant Staphylococcus aureus infection," *ACS Appl. Mater. Interfaces*, vol. 11, no. 36, pp. 32659-32669, 2019.
[13] J. Krajczewski, K. Kołątaj, and A. Kudelski, "Plasmonic nanoparticles in chemical analysis," *RSC Advances*, no. 28, pp. 17559-17576, 2017.

Tran Thi Nhung has received a B.E. degree in chemical engineering from Ho Chi Minh city University of Technology, Vietnam, in 2010; a M.E. degree in chemical engineering in Gachon University, Korea, in 2012; and a Ph.D degree in materials science and engineering in Nanyang Technological University, Singapore, in 2017. She is currently a lecturer at Ho Chi Minh city University of Technology and Education, Vietnam.
Her research focuses on the controlled synthesis of various nanomaterials for catalysis, sensing and antibacterial applications.
Email: nhungtt@hcmute.edu.vn
ORCID: https://orcid.org/0000-0003-0352-9463

Le Minh Tam has received B.E. and M.E. degrees in chemical engineering from Ho Chi Minh city University of Technology and a PhD at Max Planck Institute for Dynamics of Complex Technical Systems, Magdeburg, Germany. Postdoctoral research at Vietnam Academy of Science and Technology. Editorial Board Member of JCERU journal. Expertise in the fields of advanced materials, enantiomer separation, crystallization, chromatography, process analytical technology (PAT), chemical and bio-process engineering.
Email: tamlm@hcmute.edu.vn
ORCID: https://orcid.org/0000-0002-5372-346X